



**HAL**  
open science

# A New Modeling of Six-Phase Induction Generator for wind Turbine

S Carrière, Franck Betin, Amine Yazidi

► **To cite this version:**

S Carrière, Franck Betin, Amine Yazidi. A New Modeling of Six-Phase Induction Generator for wind Turbine. American Journal of Engineering Research (AJER), 2020, 9 (12), pp.16-23. hal-03845132

**HAL Id: hal-03845132**

**<https://u-picardie.hal.science/hal-03845132>**

Submitted on 9 Nov 2022

**HAL** is a multi-disciplinary open access archive for the deposit and dissemination of scientific research documents, whether they are published or not. The documents may come from teaching and research institutions in France or abroad, or from public or private research centers.

L'archive ouverte pluridisciplinaire **HAL**, est destinée au dépôt et à la diffusion de documents scientifiques de niveau recherche, publiés ou non, émanant des établissements d'enseignement et de recherche français ou étrangers, des laboratoires publics ou privés.



Distributed under a Creative Commons Attribution - NonCommercial 4.0 International License

## A New Modeling of Six-Phase Induction Generator for wind Turbine

S. Carrière, F. Betin, A. Yazidi

Postal address : Laboratory of Innovative Technologies, 15 avenue Francois Mitterrand, 02880 Cuffies, France

**ABSTRACT**—Nowadays, the modeling of the squirrel cage multi-phase induction generator has gained an impressive attention, especially for squirrel cage six-phase induction generator (SC6PIG). In this way, this paper proposes a fast and simple model of the SC6PIG using circuit-oriented method by the basic mathematical formulation of its generator. The proposed model associated to the current control is simulated with Simulink/MATLAB software and analyzed in healthy and faulty conditions then it is compared with the dq model and the internal circuit-oriented model. In addition, the experimental results on the test bed are provided assessing the capacities of the proposed model.

**KEYWORDS** — modeling, six-phase induction generator, current control, fault modeling

Date of Submission: 02-12-2020

Date of acceptance: 17-12-2020

### I. INTRODUCTION

Due to the decreasing of the fossil energy resources and the increasing request of electrical energy, the development of the renewable energy resources has become an emergency. One of solutions for sustainable improvement of renewable energies is the exploitation of the wind energy. For this, the kinetic energy from the wind is converted to electrical energy using a wind turbine system associated with a three-phase squirrel cage induction generator because of its robustness, simplicity, and reliability. However, one of the problems related to the three-phase induction generator is the incapacity of operating after opened phase faults on the stator windings. Indeed, when one stator winding opens or one leg of the converter is lost, due to the impossibility of controlling the remaining phases with an isolated neutral point, the induction generator has to be stopped.

One of the solutions for the faulty conditions of induction generators is to use multiphase induction generators which have more than three phases on the stator side. The most significant advantages of a multiphase induction generator [1, 2] include capability to start and run even if three active phases are remaining, the lower current per phase without an increase of voltage per phase, the lower dc link current harmonics, the higher reliability and the increased power. Among all types of multiphase induction generators, the squirrel cage six-phase induction generator (SC6PIG) is very interesting for high power wind turbines. Indeed, the SC6PIG can operate when three active phases are still remaining. This ability increases the degree of freedom in the control system of the generator.

To control the generator in healthy and faulty conditions, an accurate modeling of the SC6PIG is required. In the literature, there are some SC6PIG models, such as the  $\alpha\beta$  model obtained from transformation of a general model with Clark matrix [3] or the well-known dq model of the SG6PIG [3]. Nevertheless, problems appear in faulty operations such as failure in the stator phases or the rotor bars. Indeed, to represent these failures, it needs to modify the equations of the model and therefore it is not possible to introduce external failures in a single mathematical formulation. Therefore, an adaptive model depending on the fault type is required based on the internal circuit-oriented method [4].

Using the internal circuit-oriented model, the modeling can work properly in all different fault types and present a high accuracy. Its stator and rotor can be divided into several coils and bars, then the model can be implemented with circuit elements regarding the electrical coupling between them and calculating the mutual inductances between the coils and the bars. The computations of resistance and inductance are really complicated, especially for the SC6PIG which present a large number of coils and bars [5, 6]. In simulation, it needs a lot of computing time, then an alternative model is required.

In this paper, a novel modified circuit oriented model of the SC6PIG associated to a Proportional Integral (PI) controller as current regulation is proposed that requires less computing time than the classical circuit oriented model but that is able to simulate faulty conditions. This paper is organized as follows. Section II is devoted to the proposed model of the induction generator. The model implementation is discussed in Section III, where the model parameters, its simulation results and the current controllers are presented using MATLAB/Simulink software. Then, the results of the experimentation on the test-bed are shown in Section IV. Finally, some conclusions can be found in Section V.

## II. SC6PIG MODEL

The proposed model is arranged based on the basic voltage equations of the induction machine and the general torque and rotor speed equations which use *abcdef* axis. The squirrel-cage induction generator has a symmetrical structure, accordingly with the concentrated winding approach, and the electric angle between two consecutive phases is  $60^\circ$ .

### A. Electrical Part

The stator and rotor resistances as the inductances are constant and the stator windings are distributed sinusoidally. The stator and rotor equations of the six-phase induction machine for the proposed model, are given as :

$$[V_s] = [R_s][I_s] + \left( \frac{d[\Psi_s]}{dt} \right) = [R_s][I_s] + [emf^s] + \frac{d}{dt}([L_s][I_s]) \tag{1}$$

$$[V_r] = [R_r][I_r] + \left( \frac{d[\Psi_r]}{dt} \right) = [R_r][I_r] + [emf^r] + \frac{d}{dt}([L_r][I_r]) \tag{2}$$

$$[\Psi_s] = [L_{sr}][I_r] + [L_s][I_s] \tag{3}$$

$$[\Psi_r] = [L_{sr}]^T \cdot [I_s] + [L_r][I_r] \tag{4}$$

Where the stator and rotor voltages, the currents, the flux and the resistances, for the six stator and six rotor windings, are given as below :

$$\begin{aligned} [V_s] &= [v_{sa} v_{sb} v_{sc} v_{sd} v_{se} v_{sf}]^T \\ [V_r] &= [v_{ra} v_{rb} v_{rc} v_{rd} v_{re} v_{rf}]^T \\ [I_s] &= [i_{sa} i_{sb} i_{sc} i_{sd} i_{se} i_{sf}]^T \\ [I_r] &= [i_{ra} i_{rb} i_{rc} i_{rd} i_{re} i_{rf}]^T \\ [\Psi_s] &= [\phi_{sa} \phi_{sb} \phi_{sc} \phi_{sd} \phi_{se} \phi_{sf}]^T \\ [\Psi_r] &= [\phi_{ra} \phi_{rb} \phi_{rc} \phi_{rd} \phi_{re} \phi_{rf}]^T \\ [R_s] &= \text{diag}_6(r_s) \\ [R_r] &= \text{diag}_6(r_r) \end{aligned}$$

The flux linkages in stator and rotor are computed using :

$$\begin{bmatrix} \Psi_s \\ \Psi_r \end{bmatrix} = \begin{bmatrix} L_s & L_{sr} \\ L_{rs} & L_r \end{bmatrix} \begin{bmatrix} I_s \\ I_r \end{bmatrix} \tag{5}$$

where the stator inductance  $[L_s]$  and the rotor inductance  $[L_r]$  are given by :

$$\begin{aligned} [L_s] &= \text{diag}_6(l_s) + 3.L_{ms} \cdot [A_2(0)] \\ [L_r] &= \text{diag}_6(l_r) + 3.L_{ms} \cdot [A_2(0)] \end{aligned}$$

By assuming that both the stator and rotor are under balanced conditions, the matrix  $A_2$  is given as below (6b). The mutual inductances between the stator and the rotor are constant and depending on the position between the stator and the rotor. For the rotor windings, there are the rotor resistances, the self-inductances and the mutual inductances as in the stator windings and this matrix can be found in (6a).

$$[L_{sr}] = 3.L_{ms} \cdot [A_2(\theta_r)] = [L_{rs}]^T \tag{6a}$$

$$A_2(\theta_r) = \begin{bmatrix} \cos(\theta_r) & \cos\left(\theta_r + \frac{\pi}{3}\right) & \cos\left(\theta_r + \frac{2\pi}{3}\right) & \cos\left(\theta_r + \frac{3\pi}{3}\right) & \cos\left(\theta_r + \frac{4\pi}{3}\right) & \cos\left(\theta_r + \frac{5\pi}{3}\right) \\ \cos\left(\theta_r - \frac{\pi}{3}\right) & \cos(\theta_r) & \cos\left(\theta_r + \frac{\pi}{3}\right) & \cos\left(\theta_r + \frac{2\pi}{3}\right) & \cos\left(\theta_r + \frac{3\pi}{3}\right) & \cos\left(\theta_r + \frac{4\pi}{3}\right) \\ \cos\left(\theta_r - \frac{2\pi}{3}\right) & \cos\left(\theta_r - \frac{\pi}{3}\right) & \cos(\theta_r) & \cos\left(\theta_r + \frac{\pi}{3}\right) & \cos\left(\theta_r + \frac{2\pi}{3}\right) & \cos\left(\theta_r + \frac{3\pi}{3}\right) \\ \cos\left(\theta_r - \frac{3\pi}{3}\right) & \cos\left(\theta_r - \frac{2\pi}{3}\right) & \cos\left(\theta_r - \frac{\pi}{3}\right) & \cos(\theta_r) & \cos\left(\theta_r + \frac{\pi}{3}\right) & \cos\left(\theta_r + \frac{2\pi}{3}\right) \\ \cos\left(\theta_r - \frac{4\pi}{3}\right) & \cos\left(\theta_r - \frac{3\pi}{3}\right) & \cos\left(\theta_r - \frac{2\pi}{3}\right) & \cos\left(\theta_r - \frac{\pi}{3}\right) & \cos(\theta_r) & \cos\left(\theta_r + \frac{\pi}{3}\right) \\ \cos\left(\theta_r - \frac{5\pi}{3}\right) & \cos\left(\theta_r - \frac{4\pi}{3}\right) & \cos\left(\theta_r - \frac{3\pi}{3}\right) & \cos\left(\theta_r - \frac{2\pi}{3}\right) & \cos\left(\theta_r - \frac{\pi}{3}\right) & \cos(\theta_r) \end{bmatrix} \quad (6b)$$

**B. Mechanical Part**

The electromagnetic torque and mechanical equations that depends on the stator and the rotor currents are given by :

$$T_e = p \cdot [I_s]^T \cdot \frac{\partial [L_{sr}]}{\partial \theta_r} \cdot I_r \quad (7)$$

$$J \cdot \frac{d\Omega}{dt} + F \cdot \Omega = T_e - T_L \quad (8)$$

Where  $\Omega = \frac{1}{p} \frac{d\theta_r}{dt}$  represents the mechanical rotor speed.

**C. dq Model**

The  $\alpha\beta$  reference frame is a stationary reference frame in the stator side with the real ( $\alpha$ ) axis and the imaginary ( $\beta$ ) axis in quadrature. By decomposing the space vector voltage, current and flux, the SC6PIG equations referred on a stationary reference frame ( $\alpha\beta$ ) aligned with the stator current and the rotor flux are as following :

$$v_{sa} = R_s \cdot i_{sa} + L_s \cdot \frac{di_{sa}}{dt} + M \cdot \frac{di_{ra}}{dt} \quad (9)$$

$$v_{s\beta} = R_s \cdot i_{s\beta} + L_s \cdot \frac{di_{s\beta}}{dt} + M \cdot \frac{di_{r\beta}}{dt} \quad (10)$$

$$0 = M \cdot \frac{di_{sa}}{dt} + \omega_r \cdot M \cdot i_{s\beta} + R_r \cdot i_{ra} + L_r \cdot \frac{di_{ra}}{dt} + \omega_r \cdot L_r \cdot i_{r\beta} \quad (11)$$

$$0 = -\omega_r \cdot M \cdot \frac{di_{sa}}{dt} + M \cdot \frac{di_{s\beta}}{dt} - \omega_r \cdot L_r \cdot i_{ra} + R_r \cdot i_{r\beta} + L_r \cdot \frac{di_{r\beta}}{dt} \quad (12)$$

Then, the electric torque equation with pole pairs as p is :

$$T_e = p \cdot M \cdot (i_{s\beta} \cdot i_{r\beta} - i_{sa} \cdot i_{r\beta}) \quad (13)$$

The reference frame of the voltage equations are changed from the  $\alpha\beta$  frame (9)-(13) to the dq frame (14)-(18) by the Park transformation. Then the voltage equations are expressed as :

$$v_{sd} = R_s \cdot i_{sd} + \frac{d\phi_{sd}}{dt} - \omega_s \cdot \phi_{sq} \quad (14)$$

$$v_{sq} = R_s \cdot i_{sq} + \frac{d\phi_{sq}}{dt} + \omega_s \cdot \phi_{sd} \quad (15)$$

$$v_{rd} = 0 = R_r \cdot i_{rd} + \frac{d\phi_{rd}}{dt} - \omega_{sl} \cdot \phi_{rq} \quad (16)$$

$$v_{rq} = 0 = R_r \cdot i_{rq} + \frac{d\phi_{rq}}{dt} + \omega_{sl} \cdot \phi_{rd} \quad (17)$$

where  $\omega_{sl}$  is the slip speed defined as  $\omega_{sl} = \omega_s - \omega_r$ . In this rotating dq reference frame, the electromagnetic torque can be obtained as :

$$T_e = p \cdot \frac{M}{L_r} \cdot (i_{s\beta} \cdot \phi_{r\beta} - i_{sa} \cdot \phi_{r\beta}) \quad (18)$$

**D. Internal Circuit-Oriented Model**

The internal circuit internal equivalent (CIE model) represents the machine in the form of electrical circuits from the geometric and physical data. Moreover, this method is obtained by characterizing and assuming the electrical parameters. The parameters are such as the individual stator coils, the rotor bar meshes and the linked magnetic field between them. The method will be used to calculate the parameters of the single-phase equivalent scheme of the machine. The computation of these parameters by the model of circuit internal

equivalent method presents a wide advantage for high-power machines because the conventional tests (no-load, blocked rotor and short circuit) to deduce the parameters are no longer necessary. The circuit internal equivalent model respectively of the six-phase stator and of one mesh of rotor (between two adjacent bars) can be found in [6] and the complete explanations of this model in [4, 7, 8].

E. Proposed Model

The proposed model applying a natural "abcdef" reference frame uses the basic equations as in (1)-(6). The single-phase of this model is similar as Steinmetz or T-equivalent circuit for the six-phase induction machine. The T-equivalent circuit per phase simplified without harmonics is shown in Fig. 1, where g is the slip. An assumption is made for the modeling process, that is the parasitic effect such as the eddy currents, the magnetic field saturation and so on are neglected.

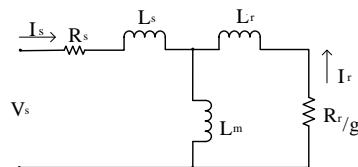


Fig. 1. Equivalent circuit

Then, the stator windings can be connected directly to an inverter or the power supply. The stator and rotor of emf equations from (1), (2), and (6) can be expressed as :

$$[emf^s] = \frac{d}{dt} ([L_{sr}] [I_r]) \tag{19}$$

$$[emf^r] = \frac{d}{dt} ([L_{rs}] [I_s]) \tag{20}$$

In the mechanical part, the inputs are the stator-rotor currents and the load torque (TL), while the outputs are the electromagnetic torque (Te) and the rotor speed (Ωr) as in (7)-(8).

III. MODEL IMPLEMENTATION

The proposed six-phase induction machine model is based on the standard equations of the induction machine (1)-(8) which are suitable to simulate stator faulty conditions. Indeed, the open circuit in the stator winding (1 to 3 phases) can be integrated by only opening switches. The proposed model (see Fig. 2) illustrates the physic components of the electrical and mechanical parts of the SC6PIG (Fig. 2).

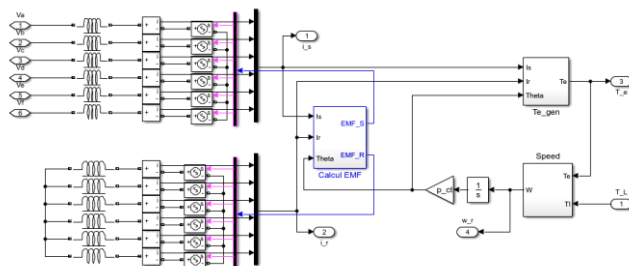


Fig. 2. The electrical parts of the SC6PIG with Simulink/MATLAB  
Fig. 3.

A. Model Parameters

The SC6PIG parameters that are given in Table I are used to simulate the machine in healthy and faulty conditions.

TABLE I. SC6PIG MODEL PARAMETERS

Rated power	24 kW
Rated voltage	230 V
Rated speed	13.09 rad/s
Stator resistance	0.262 Ω
Rotor resistance	0.64 Ω
Stator leakage inductance	3.8 mH
Rotor leakage inductance	2.4 mH
Mutual inductance	26.3 mH
Friction coefficient	21.39 N.m/rad/s
Inertia coefficient	704 kg.m <sup>2</sup>

**B. Simulation Results**

The simulation tests using Simulink/MATLAB software have been realized in no-load conditions from 0s to 2.35s and in load conditions (-2930 Nm) from 2.35s to 4.5s. The initial rotor speed is set to 13.09 rad/s corresponding to the stator synchronous speed. The rotor speed at steady state is at no-load at 13.06 rad/s and in load at 13.33 rad/s.

Fig.3 represents the phase a stator current with the dq model, the CIE model and the proposed model. The dq model and the proposed model results present the same magnitude around 25.3A (no-load) and 45.4A (load).

Fig. 4 depicts the electromagnetic torque using the dq model, the CIE model and the proposed model. At steady state, the electromagnetic torque, whatever the model, is around 279 Nm in no-load conditions and around -2645 Nm in load conditions [6]. Comparing the torque simulation results of the dq model, the CIE model, and the proposed model, the performances of both of them are summarized in Table II.

Of course, the execution time depends on the laptop configuration. For a core i7 @1.90GHz with 12.0GB memory, the shortest execution time of the 4.5s motion is obtained with the dq model (36s), while the CIE model and the proposed model require respectively 20h2min5s and 17min59s.

**TABLE II.** COMPARISON OF TORQUE RESPONSES WITH DQ MODEL, CIE MODEL AND PROPOSED MODEL

Model		dq	CIE	Proposed
Time execution (s)		36s	20h2min5s	17min59s
Overshoot	at t= 0s	1818	975	1816
	at t=2.35s	-2623	-1498	-2624
Rise time (s)	at t= 0s	0.016	0.011	0.016
	at t=2.35s	0.078	0.071	0.079

Another test is the comparison between the CIE model and the proposed model results under healthy and faulty conditions. In the stator opened winding case, the proposed model can work as circuit-oriented model by opening or closing a switch. In this paper, the model simulation results with up to two opened phases are given. Fig. 5 illustrates the transient and steady state responses with both the CIE model and the proposed model in healthy and faulty conditions. For this test, the generator is in healthy condition until t=1s, then phase a is opened (from t=1s to t=2s) and finally phases a and b are opened (t=2 to t=3s). As shown in Fig. 5a and 5b, the magnitude rates of the stator currents in healthy condition between the CIE model and the proposed model present some differences about 9%. With the CIE model, it required more time than with the proposed model to reach the steady state since the transient times with the CIE model and the proposed model are about 1 s and 0.4s respectively. In faulty conditions, the torque response of the proposed model presents less oscillations than the CIE model (about 50% for missing phase a and about 30% for missing phases a-b).

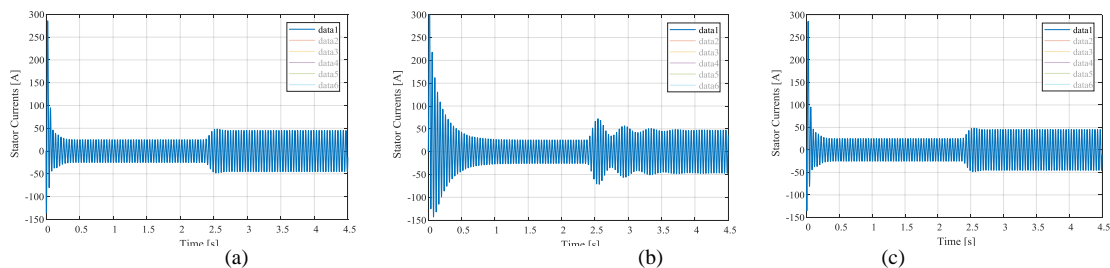


Fig. 3. Simulated stator currents from start-up to steady state: (a) dq model, (b) CIE model, (c) proposed model.

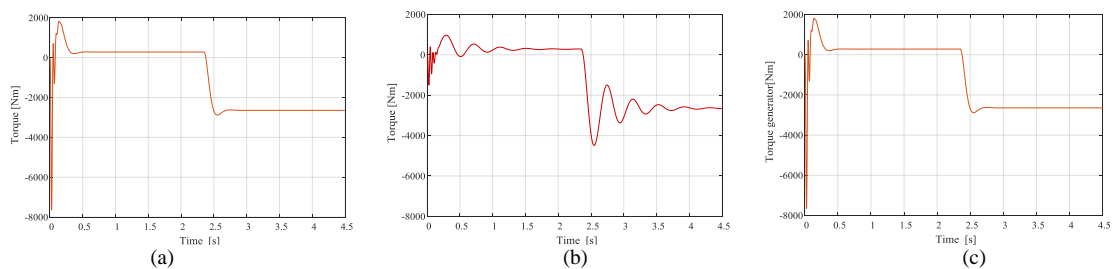


Fig. 4. Simulated torque from start-up to steady state: (a) dq model, (b) CIE model, (c) proposed model.

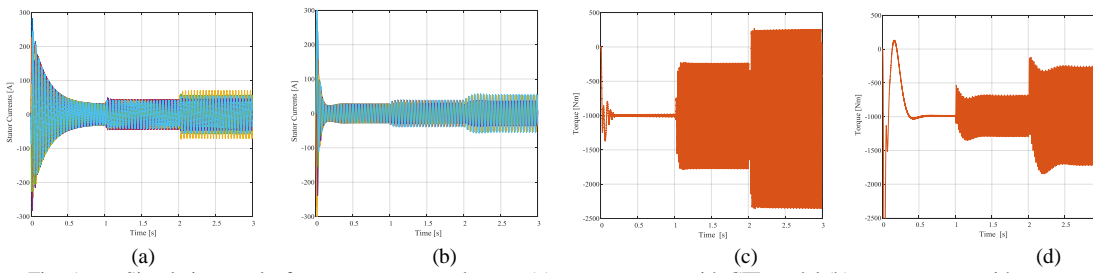


Fig. 5. Simulation results from start-up to steady state:(a) stator currents with CIE model,(b)stator currents with proposed model, (c)torque with CIE model, (d)torque with proposed model

The models in the dq axis, with the circuit internal equivalent method and with the proposed model have been studied in healthy conditions. Each model present different advantages. Indeed, the dq model is useful for the controller design. However, with the stator and rotor coil connections of the dq model, it is really difficult to simulate faults since the parameters of the model equations have to be modified. The most accurate model of the SC6PIG is the CIE model since it integrates every stator and rotor components. This model is more suitable for winding failures simulation. Nevertheless, it has a wide drawbacks since it requires a large amount of computations that induces a long time of execution. The proposed model is simpler than the CIE model since it uses the mathematical formulation of the SC6PIG and therefore it requires less execution time than the CIE model while it can also simulate electrical faults. It is a good compromise between precision and execution time.

**IV. EXPERIMENTAL RESULTS (COMPARISON)**

The SC6PIG model is now simulated with a currents control based on the Indirect Rotor Field Oriented Control (IRFOC) as shown on Fig. 6. Indeed, the currents control contains two stator currents control loops both for  $i_{sd}$  and  $i_{sq}$ . The Clarke and Park ( $T_2$  and  $T_6$ ) matrices are used to convert the vectors from the abcdef reference frame to the  $\alpha\beta\gamma$  reference frame, then to dqz reference frame. In this paper, the control is made only on the dq axis and ignores the z axis. The inputs and outputs of the current controllers are respectively  $i_{sdq}$  and  $V_{sdq}$ .

To achieve the stator currents control of the SC6PIG, the controller uses Proportional-Integrator (PI) controller. Furthermore, when one, two or three phases are opened, some modifications have to be realized in the current control loop. These modifications include the transformation matrix for stator and rotor windings, as  $T_6$  matrix and the parameters of the PI controller [7] using Table III [8].

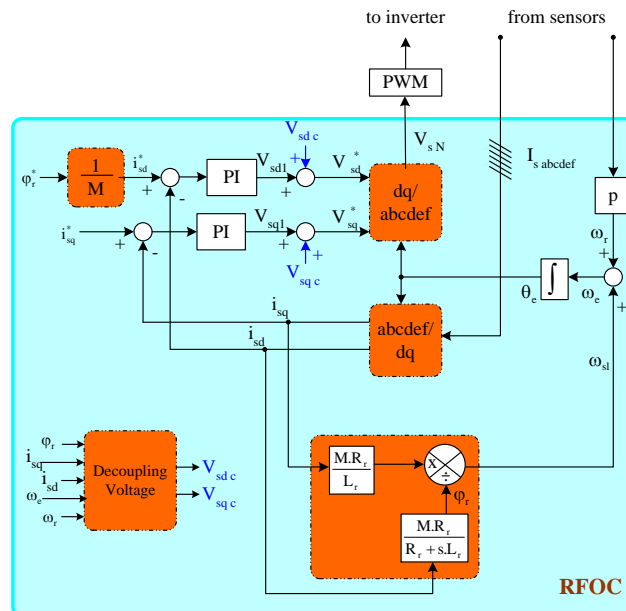


Fig. 6. RFOC scheme

**TABLE III.** MODIFIED OF MACHINE INDUCTANCES

Condition	$L_{s\alpha}$	$L_{s\beta}$	$M_{\alpha}$	$M_{\beta}$
Healthy	$l_s+3l_{ms}$	$l_s+3l_{ms}$	$3l_{ms}$	$3l_{ms}$
Faulty in phase a	$l_s+3l_{ms}$	$l_s+2l_{ms}$	$3l_{ms}$	$2.4495l_{ms}$

To verify the proposed model of the SC6PIG, an experimental test-bed (Fig. 7) has been developed as close as possible to a real wind turbine using a six-phase induction machine. This test bed is composed of a 45kW 3-phase induction machine (3PIM) connected to a gearbox to emulate the wind force (from 0 to 133 rpm), a dynamic torque meter and the 6PIG. The position is measured via an optical encoder with a 4096 pulse per revolution. The power is extracted through two back-to-back converters of 15kVA each with their dc bus connected. These converters are controlled by an industrial computer programmed in real time with MATLAB/Simulink<sup>®</sup> software. The currents and dc bus voltages are measured at 10kHz sampling frequency.

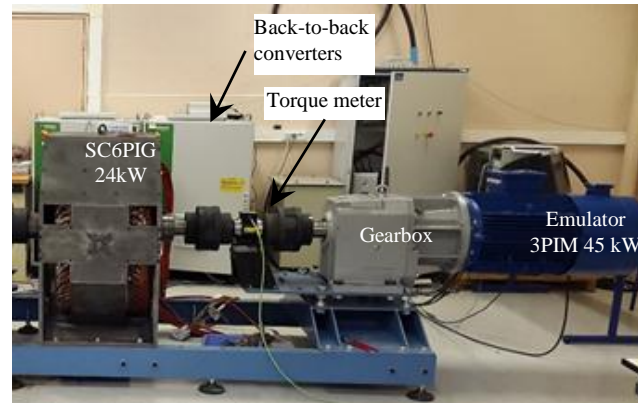


Fig. 7: Experimental test bed

The simulation results are obtained with a simulation step of  $1\mu\text{s}$  while the reference signal of the rotor flux is fixed to  $2\text{Wb}$  and the reference signal of the quadrature current is  $-15\text{A}$ .

Fig 8 represents the simulation with the proposed model and the experimental results in the healthy mode while Fig 9 depicts them when the phase a is missing.

Fig. 8.a and 8.b represent the simulated and experimental results for the stator currents in healthy condition. The magnitudes of these signals are the same for each phase. Indeed, the average values for the simulation and experimentation results are around  $18.5\text{A}$  and  $18.1\text{A}$  respectively. Fig. 8.c to 8.f illustrate the  $I_d$  and  $I_q$  which are around  $25.4\text{A}$  and  $-15\text{A}$  in simulation and around  $25.3\text{A}$  and  $-15\text{A}$  in experimentation.

The electromagnetic power obtained in simulation (Fig. 8.g) and in experimentation (Fig. 8.h) show that the ripples of the power are around  $0.17\text{ kW}$  and  $0.15\text{ kW}$  in healthy condition.

Fig. 9.a and 9.b represent the simulated and experimental results of the stator currents while Fig. 9.c to 9.f depict the  $I_d$  and  $I_q$  currents in simulation and experimentation when the phase a is missing. The  $I_d$  and  $I_q$  values are around  $28\text{A}$  and  $-15\text{A}$  in simulation and around  $28.1\text{A}$  and  $-15\text{A}$  in experimentation. The electromagnetic power obtained in simulation (Fig. 9.g) and in experimentation (Fig. 9.h) show that the power value oscillates around  $4.15\text{ kW}$  in simulation and  $4.14\text{ kW}$  in experimentation.

From the comparison between simulation and experimental results, we can claim that the proposed model is accurate in healthy and faulted mode without requiring large execution time.

## V. CONCLUSION

This paper proposes a faster and simpler circuit-oriented model based on a basic mathematical model of the six-phase induction machine. For simulation, the proposed model uses a natural "abcdef" reference frame with the induction machine parameters as for the dq model and utilizes the property of Simscape Power Systems to represent the electrical parts of the SC6PIG. It can be used in healthy condition and in faulty conditions when there are up to three opened stator phases. For a  $24\text{kW}$  SC6PIG, the execution time of the proposed model is faster than the CIE model. The simulation and experimental results with the PI current controllers associated to FOC are really close. The proposed model is really suitable to simulate the dynamics of the SC6PIG since it does not require large execution time and is able to simulate dynamics in healthy and faulty conditions.



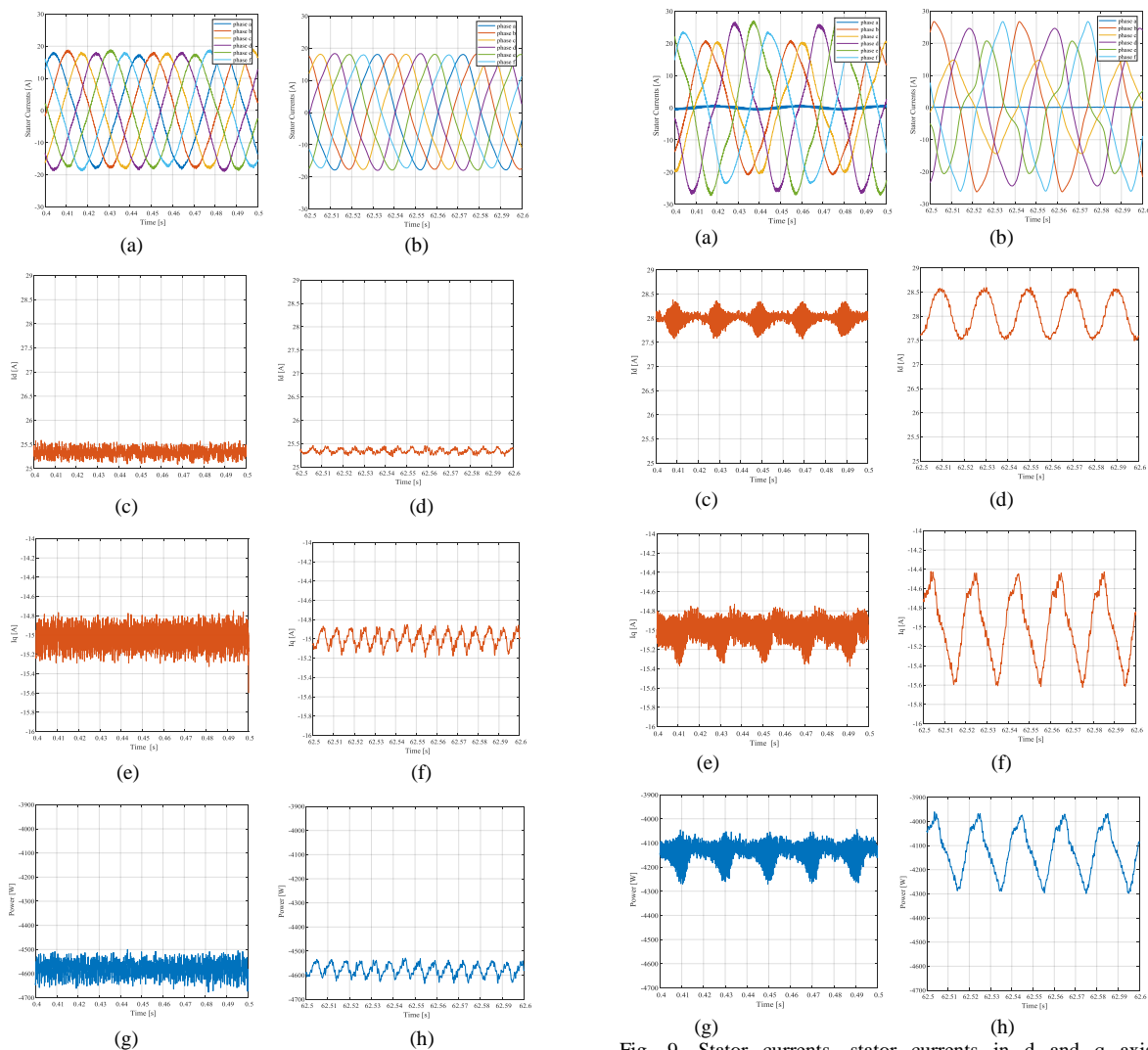


Fig. 8. Stator currents, stator currents in d and q axis, electromagnetic power in healthy conditions. (a), (c), (e), and (g) Simulation results. (b), (d), (f), and (h) Experimental results

Fig. 9. Stator currents, stator currents in d and q axis, electromagnetic power in faulty conditions phase a. (a), (c), (e), and (g) Simulation results. (b), (d), (f), and (h) Experimental results

REFERENCES

- [1] T. A. Lipo, "d-q Model For Six Phase Induction Machines," in *International Conference on Electrical Machine*, Athens, Greece, 1980, pp. 860-867.
- [2] E. Levi, R. Bojoi, F. Profumo, H. A. Toliyat, and S. Williamson, "Multiphase induction motor drives - a technology status review," *IEE Proceedings - Electric Power Applications* vol. 1, pp. 489-516, 2007.
- [3] R. Kianinezhad, B. Nahid-Mobarakeh, L. Baghli, F. Betin, and G. A. Capolino, "Modeling and Control of Six-Phase Symmetrical Induction Machine Under Fault Condition Due to Open Phases," *IEEE Transactions on Industrial Electronics*, vol. 55, pp. 1966-1977, 2008.
- [4] A. Pantea, A. Yazidi, F. Betin, M. Taherzadeh, S. Carriere, H. Henao, and G. Capolino, "Six-Phase Induction Machine Model for Electrical Fault Simulation Using the Circuit-Oriented Method," *IEEE Transactions on Industrial Electronics*, vol. 63, pp. 494-503, 2016.
- [5] G. Aroquiadassou, H. Henao, G. A. Capolino, A. Boglietti, and A. Cavagnino, "A simple circuit-oriented model for predicting six-phase induction machine performances," in *Annual Conference on IEEE Industrial Electronics (IECON)*, 2006, pp. 1441-1446.
- [6] A. Pantea, A. Yazidi, F. Betin, S. Carriere, B. Vacossin, H. Henao, and G. Capolino, "Low speed six-phase induction generator model for wind turbines," in *IEEE International Electric Machines and Drives Conference (IEMDC)*, 2017, pp. 1-6.
- [7] M. Taherzadeh, S. Carriere, M. Joorabian, F. Betin, R. Kianinezhad, and G. A. Capolino, "On-line observer modification of a six-phase induction generator in faulted mode," in *Annual Conference on IEEE Industrial Electronics (IECON)*, 2015, pp. 001477-001482.
- [8] A. Pantea, A. Yazidi, F. Betin, S. Carrière, A. Sivert, B. Vacossin, H. Henao, and G. Capolino, "Fault-Tolerant Control of a Low-Speed Six-Phase Induction Generator for Wind Turbines," *IEEE Transactions on Industry Applications*, vol. 55, pp. 426-436, 2019